$A_2BiI_5O_{15}$ ($A=K^+$ or Rb^+): Two New Promising Nonlinear Optical Materials Containing $[I_3O_9]^{3-}$ Bridging Anionic Group †

Yin Huang[a], Xianggao Meng[b], Pifu Gong[c], Lei Yang,[c] Zheshuai Lin[c] Xingguo Chen[a] and Jingui Qin*[a]

[a]Department of Chemistry, Wuhan University, Wuhan 430072, China,

[b]College of Chemistry, Central China Normal University, Wuhan 430079, China

[c] Beijing Center for Crystal R&D, Technical Institute of Physics and Chemistry, Chinese Academy of Sciences, Beijing 100190, China

$K_2BiI_5O_{15}$ and $Rb_2BiI_5O_{15}$ are synthesized and contain a unique $[I_3O_9]^{3-}$ bridging anionic group. Their powders show phase-matchable SHG effect 3 times that of KDP and the laser damage thresholds of 84 and 72 MW/cm^2, plus wide transparent range and good thermal stability.

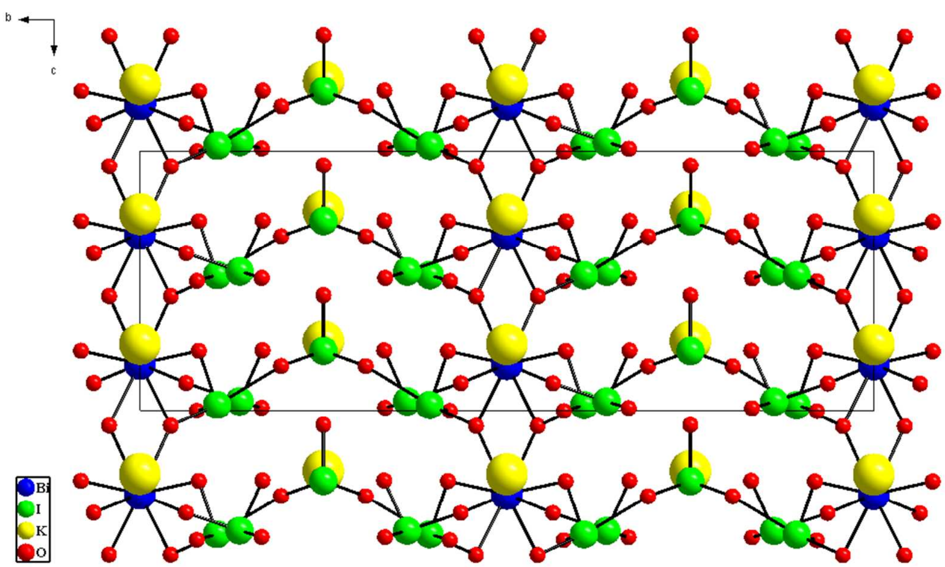

Journal Name

RSCPublishing

ARTICLE

Cite this: DOI: 10.1039/x0xx00000x

Received 00th January 2012,
Accepted 00th January 2012

DOI: 10.1039/x0xx00000x

www.rsc.org/

$A_2BiI_5O_{15}$ ($A=K^+$ or Rb^+): Two New Promising Nonlinear Optical Materials Containing $[I_3O_9]^{3-}$ Bridging Anionic Groups †

Yin Huang, [a] Xianggao Meng, [b] Pifu Gong, [c] Lei Yang,[c] Zheshuai Lin, [c] Xingguo Chen [a] and Jingui Qin [*a]

Two new alkali metal bismuth iodates, $K_2BiI_5O_{15}$ and $Rb_2BiI_5O_{15}$, have been synthesized by hydrothermal method. They are isostructural with the same noncentrosymmetric (NCS) orthorhombic space group Abm2 and contain a unique $[I_3O_9]^{3-}$ bridging anionic group. Their powders showed phase-matchable second-harmonic generation (SHG) effect 3 times that of KH_2PO_4 (KDP) and the laser-induced damage threshold values of 84 and 72 MW/cm^2, respectively. They also exhibit a wide transparent range (up to 12 μm) and good thermal stability (450 °C).

Introduction

Second-order nonlinear optical (NLO) crystal materials have played a very important role in the laser technology, such as laser frequency conversion, optical parameter oscillators, and signal communication.[1] In the past decades, some important NLO crystals have been found in the UV and visible regions, such as β-BaB_2O_4 (BBO), LiB_3O_5 (LBO), KH_2PO_4 (KDP), $KTiOPO_4$ (KTP) and $LiNbO_3$ (LN).[2] In the infrared (IR) region, many current NLO crystals such as $AgGaS_2$, $AgGaSe_2$ and $ZnGeP_2$,[3] have been reported. However, these chalcogenide crystals exhibit low laser damage thresholds (LDT), and their applications are heavily hindered. Many factors may cause laser damage. Two main strategies to increase LDT are to improve the crystal quality and to enlarge the band gap of the materials. It is believed that small band gaps of the semiconductor chalcogenides are intrinsic reason for their low LDT. Therefore, the search for new IR NLO crystals with wide band gap has become one of the great challenges in this field.

Recently, a series of metal iodates with good performance have become an important class of visible and IR NLO materials, including NaI_3O_8, α-$Cs_2I_4O_{11}$, $La(IO_3)_3$, $AMoO_3(IO_3)$ (A = Rb, Cs), $LiMoO_3(IO_3)$, $A_2Ti(IO_3)_6$ (A = Li, Na), $BaNbO(IO_3)_5$, $K(VO)_2O_2(IO_3)_3$, $BiO(IO_3)$ and $Bi_2(IO_4)(IO_3)_3$ among the others.[4,5] One of the reasons for large SHG response is due to the stereochemically active lone electron pair on the I (V) atom.

Among the above iodates the bismuth iodates are quite interesting because both Bi^{3+} and I^{5+} are heavy metal cations containing a lone electron pair, and are favorable for a large SHG response and a wide transparent range. Recently, Halasyamani's group and Hu's group have reported two bismuth iodates, $BiO(IO_3)$ and $Bi_2(IO_4)(IO_3)_3$.[5] They display strong SHG responses of 12.5 and 5 times that of KDP, respectively.

We have specially been interested in alkali metal bismuth iodates, since we think that the existences of alkali metal cations will strengthen the ionic nature of bismuth iodates and this may help improve the LDT. In this paper we report the synthesis, crystal structure and NLO property of two alkali metal bismuth iodates, $K_2BiI_5O_{15}$ and $Rb_2BiI_5O_{15}$. It was found that their crystals contain $[I_3O_9]^{3-}$ bridging anionic groups, that have never been reported before. Both crystals are noncentrosymmetric and isostructural. They not only show a moderately strong SHG response of 3 times as strong as that of KDP, but also exhibit the LDT as high as 84 and 72 MW/cm^2, respectively, higher than that of $AgGaS_2$, a commercially available IR NLO crystal. In addition, they also exhibit wide transparent range and good thermal stability. These results indicate that they are two promising candidates for NLO materials in the IR region.

Experimental

Materials and Instruments

All of the chemicals were analytically pure from commercial sources and used without further purification.

Powder X-ray diffraction (XRD) patterns of polycrystalline material were collected on a Bruker D8 Advanced diffractometer with Cu-Kα radiation (λ = 1.54186 Å) in the range of 10°-70° (2θ) at a scanning rate of 6°/min.

Energy dispersive X-ray spectroscopy (EDX) was performed on FEI Quanta 200 scanning electron microscope (SEM) equipped with X-ray spectroscope.

The optical transmission spectra in the mid-IR region were recorded on a NICOLET 5700 Fourier-transformed infrared (FT-IR) spectrophotometer in the 4000-700 cm^{-1} region (2.5-14 μm) using the attenuated total reflection (ATR) technique with a germanium crystal.

The UV-vis diffuse reflectance spectra were measured on a Varian Cary 5000 UV-vis-NIR spectrophotometer in the region of 200-1000 nm. A $BaSO_4$ plate was used as the standard (100% reflectance), on which the finely ground samples from the crystals were coated. The absorption spectrum was calculated from the reflectance spectra using the Kubelka-Munk function: $\alpha/S = (1-R)^2/2R$,[6] where α is the absorption coefficient, S is the scattering coefficient, and R is the reflectance.

The measurements of second harmonic generation (SHG) were carried out on the sieved powder samples by using the Kurtz and Perry method[7] with a 1064 nm Q-switched Nd: YAG laser. Microcrystalline KDP served as the standard. Laser-induced damage threshold (LDT) was measured on powder samples (grounded crystals placed between two glass sheets), with the laser source (1064 nm, 5 ns, 1 Hz). The title compounds and $AgGaS_2$ were sieved into the same particle size range (100 - 200 μm). The energy of the laser emission was gradually increased until the colour of the samples changed.[4a, 8]

The thermogravimetric analysis (TGA) was carried out with a Netzsch STA 449c analyzer. The crystal sample was added into an Al_2O_3 crucible and heated from 30 °C to 800 °C at a heating rate of 10 K/min under flowing N_2.

Synthesis

These two compounds were synthesized by the same method. Their single crystals were synthesized by the hydrothermal reaction.

$K_2BiI_5O_{15}$: KIO_4 (1.3800 g, 6 mmol), KCl (0.4473 g, 6 mmol), Bi_2O_3 (0.4660 g, 1 mmol), H_5IO_6 (1.3676 g, 6 mmol) and 3mL of deionized water were sealed in a 23 mL Teflon-lined autoclave. The autoclave was gradually heated to 230 °C, held for 4 days, and cooled slowly to 30 °C at a rate of 3 °C/h. The product was washed with water in an ultrasonic cleaner and then dried in air. The colourless rod-like crystals of $K_2BiI_5O_{15}$ were collected in a yield of about 69 % based on Bi. Its purity was confirmed by X-ray powder diffraction analysis (Fig. S1, ESI†). The EDX analysis of $K_2BiI_5O_{15}$ provided a K: Bi: I ratio of 2.0: 1.0: 4.7, which is close to that determined from single-crystal X-ray diffraction analysis (Fig. S2, ESI†).

$Rb_2BiI_5O_{15}$: $RbIO_4$ (1.6582 g, 6 mmol, prepared by reaction of Rb_2CO_3 with H_5IO_6), RbCl (0.7255 g, 6 mmol), Bi_2O_3 (0.4660 g, 1 mmol), H_5IO_6 (1.3676 g, 6 mmol) and 3mL of deionized water were sealed in a 23 mL Teflon-lined autoclave. Then the operation procedures are the same as those for the synthesis of $K_2BiI_5O_{15}$. The colourless rod-like crystals of $Rb_2BiI_5O_{15}$ were collected in a yield of about 60 % based on Bi. Its purity was confirmed by X-ray powder diffraction analysis (Fig. S3, ESI†). The EDX analysis of $Rb_2BiI_5O_{15}$ provided a Rb: Bi: I ratio of 2.1: 1.0: 4.8, which is close to that determined from single-crystal X-ray diffraction analysis (Fig. S4, ESI†).

Single Crystal Structure Determination

Single crystal of $K_2BiI_5O_{15}$ and $Rb_2BiI_5O_{15}$ with dimensions of 0.10 x 0.10 x 0.10 mm^3 and 0.10 x 0.05 x 0.05 mm^3, respectively, were selected and used for single-crystal diffraction experiment. Data sets were collected with a Bruker APEX DUO diffractometer equipped with a CCD detector (graphite-monochromated Mo Kα radiation λ = 0.71073 Å) at 298(2) K. Data sets reduction and integration were performed using the software package SAINT PLUS.[9] The crystal structure is solved by direct methods and refined using the SHELXTL 97 software package.[10] Crystallographic data for $K_2BiI_5O_{15}$ and $Rb_2BiI_5O_{15}$ are summarized in Table 1. The selected bond distances for $K_2BiI_5O_{15}$ and $Rb_2BiI_5O_{15}$ are listed in Table S1 and S2 (ESI†). Their CCDC numbers are 963741 and 963742, respectively.

Computational Method

The first-principles electronic structure calculations for $K_2BiI_5O_{15}$ and $Rb_2BiI_5O_{15}$ are performed using the plane-wave pseudopotential method[11] implemented in CASTEP package.[12] The optimized norm-conserving pseudopotentials[13] in the Kleinman-Bylander form[14] for all the elements are used, in which K $3s^23p^64p^1$, Rb$4s^24p^65p^1$, Bi $5d^{10}6s^26p^3$, I $5s^25p^5$, and O $2p^22p^4$ electrons are treated as the valence electrons, respectively. The Perdew, Burke and Ernzerhof (PBE) functionals[15] of generalized gradient approximation (GGA) are adopted to describe the exchange-correlation (XC) functionals. The kinetic energy cutoffs of 550 eV and Monkhorst-Pack *k*-point meshes[16] with a density of 3×3×2 points in the Brillouin zone are chosen. Our tests reveal that the above computational set ups are sufficiently accurate for present purposes.

Table S1. Crystallographic data for $K_2BiI_5O_{15}$ and $Rb_2BiI_5O_{15}$

Formula	$K_2BiI_5O_{15}$	$Rb_2BiI_5O_{15}$
Formula weight	1161.68	1254.42
Temperature (K)	298(2)	298(2)
Crystal system	Orthorhombic	Orthorhombic
Space group	Abm2	Abm2
a (Å)	8.2115(5)	8.2257(6)
b (Å)	23.2072(15)	23.5398(18)
c (Å)	8.1977(5)	8.2544(6)
V ($Å^3$)	1562.20(17)	1598.3(2)
Z	4	4
Density (calculated) (Mg/m^3)	4.939	5.213
Absorption coefficient (mm^{-1})	21.774	26.813
F(000)	2024	2168
Crystal size (mm^3)	0.10 x 0.10 x 0.10	0.10 x 0.05 x0.05
Reflections collected	4867	7999
Independent reflections	1470 [R(int) = 0.0262]	2510 [R(int) = 0.0340]
Data / restraints / parameters	1470 / 1 / 111	2510 / 13 / 111
Goodness-of-fit on F^2	1.058	1.068
Final R indices [I>2sigma(I)][a]	R_1=0.0169, wR_2= 0.0418	R_1=0.0399, wR_2= 0.1099
R indices (all data)	R_1=0.0169, wR_2=0.0419	R_1=0.0403, wR_2= 0.1104

[a] $R_1 = \sum||F_o| - |F_c|| / \sum|F_o|$, $wR_2 = \{\sum[w(F_o^2 - F_c^2)^2] / \sum w[(F_o)^2]^2\}^{1/2}$.

Based on the electronic structures, the refractive indices and birefringence in $K_2BiI_5O_{15}$ and $Rb_2BiI_5O_{15}$ are predicted by considering the electronic transition between valance band (VB) and conduction band (CB).[17] Moreover, the SHG coefficients d_{ij} are obtained by the formula developed by Lin et al,[18] and then the power SHG effects are determined by the Kurtz-Perry method. [7] It is well acknowledged that the DFT calculations with the PBE functional always underestimate the energy band gap of crystals. For calculating the optical coefficients, a scissors operator[19] is usually introduced to shift up all the conduction bands to agree with the measured band gap.

Results and Discussions

Hydrothermal reactions of KIO_4 (or $RbIO_4$), Bi_2O_3, KCl (or RbCl) and H_5IO_6 afforded two new alkali metal bismuth iodates $K_2BiI_5O_{15}$ and $Rb_2BiI_5O_{15}$. They represent the first two compounds in the A-Bi-I-O (A= alkali metal) systems. In addition, we have tried using $BiCl_3$ to replace Bi_2O_3 as starting material and we can also obtain the target material.

Crystal Structural Descriptions

$K_2BiI_5O_{15}$ and $Rb_2BiI_5O_{15}$ were synthesized by hydrothermal reactions of a mixture of KCl (or RbCl), KIO_4 (or $RbIO_4$), Bi_2O_3, and H_5IO_6 in 3mL H_2O at 230 °C for 4 days. Single crystal structural analysis indicates that $K_2BiI_5O_{15}$ and $Rb_2BiI_5O_{15}$ are isostructural, with the same noncentrosymmetric orthorhombic space group Abm2 (No.39). Therefore, we only need to describe the structure of $K_2BiI_5O_{15}$ as an example. The asymmetric unit contains two crystallographically independent K atoms, one independent Bi atom, three independent I atoms, and eight independent O atoms. The view of crystal structure of $K_2BiI_5O_{15}$ down the a-axis is shown in Fig. 1. Each Bi atom is eight-coordinated by eight O atoms to form the BiO_8 polyhedron with the Bi-O distances ranging from 2.352(5) to 2.549(4) Å. Two adjacent BiO_8 polyhedra are connected by two O2 atoms to form chain structure along the c-axis (Fig. 2). On the other hand, along b-axis, every BiO_8 chain is connected to the neighbouring two BiO_8 chains through $[I_3O_9]^{3-}$ bridges, respectively (Fig. 3c). This $[I_3O_9]^{3-}$ bridge is first found in iodates. It is formed by connecting three $[IO_3]$ trigonal pyramids (two $[I(1)O_3]$ as the terminals and one $[I(3)O_3]$ in the centre) through two O7 atoms (Fig. 3b). The $[I_3O_9]^{3-}$ bridge is a noncentrosymmetric unit and they are arranged with the same direction along the c-axis (Fig. 3c). So the $[I_3O_9]^{3-}$ bridges can produce a dipole moment along the c-axis. As a result, $K_2BiI_5O_{15}$ should exhibit second order NLO effect.

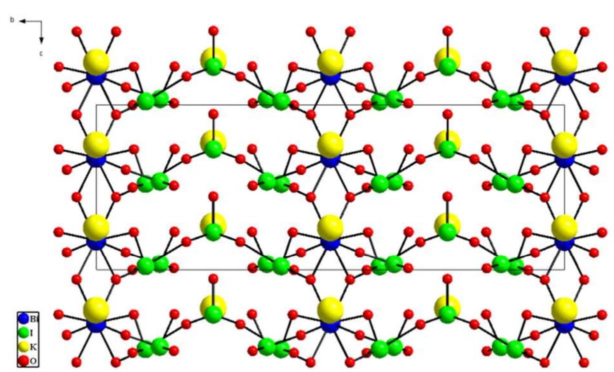

Fig.1 View of crystal structure of $K_2BiI_5O_{15}$ down the a-axis.

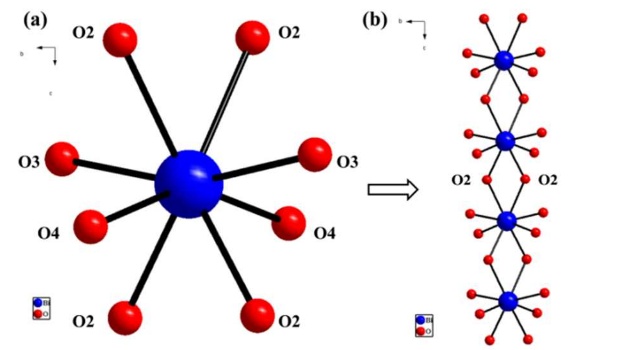

Fig.2 The structure of BiO_8 polyhedron (a); the chain structure of BiO_8 (b).

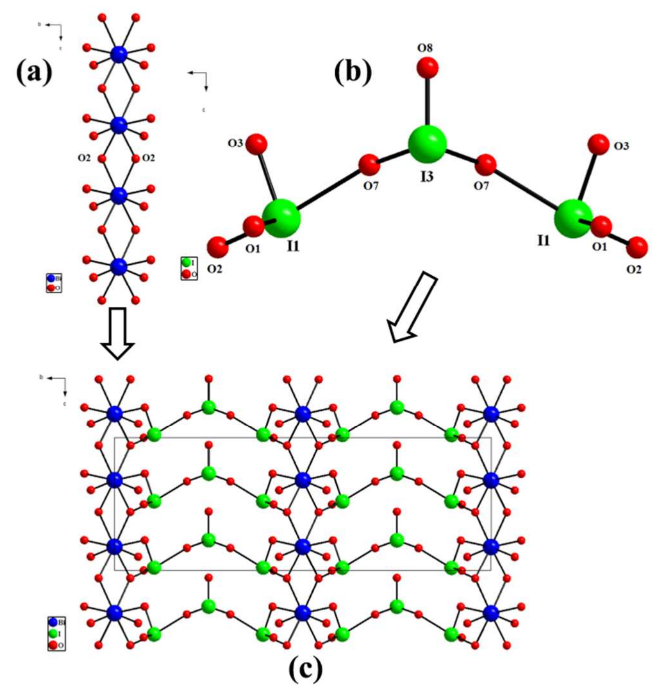

Fig.3 The chain structure of BiO_8 polyhedra (a); the structure of $[I_3O_9]^{3-}$ bridging anionic group (b); the I structure composed of the BiO_8 chain and $[I_3O_9]^{3-}$ bridge.

ATR-FTIR and UV-vis Spectra

The ATR-FTIR spectra of $K_2BiI_5O_{15}$ and $Rb_2BiI_5O_{15}$ indicate that the transparent regions of their powders in the range of 4000-816cm^{-1} (2.5-12 μm) (see Fig. S7 and S8, ESI†). The peak of 816cm^{-1} can be assigned to I-O vibrations.[4] The UV-vis absorption spectra and optical diffuse reflectance spectra of them show that their absorption edges are at 354 and 351 nm, respectively indicating that the optical band gaps of $K_2BiI_5O_{15}$ and $Rb_2BiI_5O_{15}$ are 3.50 and 3.53 eV, respectively (Fig. 4 and 5). As it is well known that the band gaps have great influence on the laser damage threshold. These band gaps imply that $K_2BiI_5O_{15}$ and $Rb_2BiI_5O_{15}$ should have a considerable laser damage threshold.

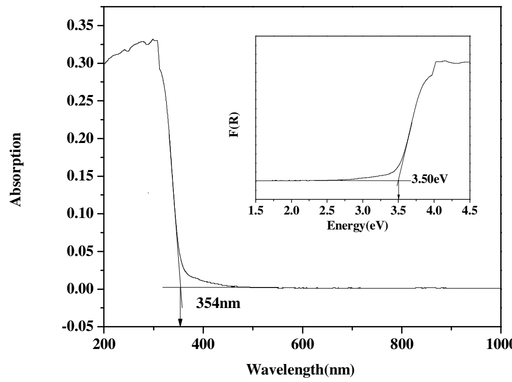

Fig. 4 UV-vis absorption spectrum; and the inset is optical diffuse reflectance spectrum of $K_2BiI_5O_{15}$.

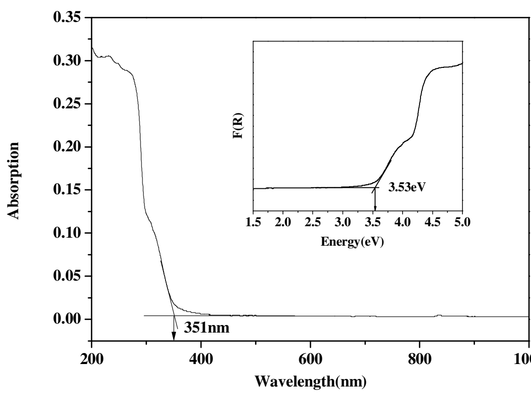

Fig. 5 UV-vis absorption spectrum; and the inset is optical diffuse reflectance spectrum of $Rb_2BiI_5O_{15}$.

NLO Property and LDT Measurement

Powder SHG measurements using 1064 nm radiation revealed that they showed SHG efficiencies approximately of about 3 times as strong as that of KDP. The tendency of the curve indicates that $K_2BiI_5O_{15}$ and $Rb_2BiI_5O_{15}$ belong to the phase-matchable class, [7] which is a very important character of NLO material for the laser harmonic generation (Fig. 6 and 7).

A preliminary measurement of the laser-induced damage threshold (LDT) has been carried out on powder samples with the powders of $AgGaS_2$ as the reference. The results indicate that $K_2BiI_5O_{15}$ and $Rb_2BiI_5O_{15}$ exhibit the LDT values of 84 and 72 MW/cm^2 (1064nm, 5ns), respectively. While in the same measurement conditions, $AgGaS_2$ powders show LDT of 5.2 MW/cm^2.

It seems to be worth to compare and discuss on the structure and properties of $BiO(IO_3)$ and $Bi_2(IO_4)(IO_3)_3$ with our new compounds, $K_2BiI_5O_{15}$ and $Rb_2BiI_5O_{15}$. They are four noncentrosymmetric iodates containing bismuth (III) and showing SHG effects. Firstly, their similarities are that all contain both iodine (V) and bismuth (III) with lone electron pairs, and that the NLO effects of these four iodates mainly come from the contributions of the polarized iodate groups. Secondly, each compound exhibits special feature in the crystal structure. In the crystal of $BiO(IO_3)$, the layers of $[Bi_2O_2]^{2+}$ cationic groups are connected to isolated $[IO_3]^-$ anions. All of the $[IO_3]^-$ groups are aligned in the same direction to produce a strong SHG response of 12.5 × KDP. Crystal of $Bi_2(IO_4)(IO_3)_3$ contains a three-dimensional dimensional framework through a combination of the IO_3, IO_4, BiO_8, and BiO_9 polyhedra. It is the first noncentrosymmetric structure with $[IO_4]^{3-}$ anions, and produces a moderately strong SHG response of 5 × KDP. The two title compounds are the first two alkali metal bismuth iodates. Compared with $BiO(IO_3)$ and $Bi_2(IO_4)(IO_3)_3$, their powders SHG efficiencies become smaller, but their optical band gaps become larger. This is favourable for improving the LDT. On the other hand, our two compounds are the first bismuth iodates that contain alkali metal cations. Their crystals contain the unique $[I_3O_9]^{3-}$ bridging anionic groups responsible for showing a SHG response of 3 × KDP. Thirdly, their main difference is the absence or presence of alkali metal cations in the molecules. The optical band gaps of both $BiO(IO_3)$ and $Bi_2(IO_4)(IO_3)_3$ are 3.3 eV, while our two alkali metal bismuth iodates exhibit a little higher optical band gaps of 3.50 eV and 3.53 eV, and their powders LDT have reached 84 and 72 MW/cm^2, respectively. The results seem to have supported our expectation that the existence of alkaline metal cations will strengthen the ionic nature of bismuth iodates so as to increase the LDT value, though their SHG may be a little weaker.

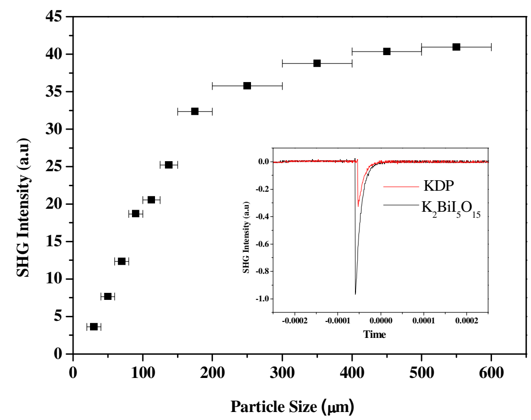

Fig. 6 The phase-matching curve for $K_2BiI_5O_{15}$; and the inset is Oscilloscope traces of the SHG signals for the powders (100 - 125 μm) of KDP and $K_2BiI_5O_{15}$.

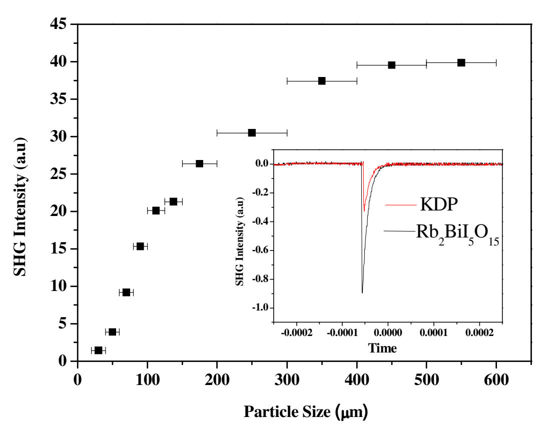

Fig. 7 The phase-matching curve for $Rb_2BiI_5O_{15}$; and the inset is Oscilloscope traces of the SHG signals for the powders (100 - 125 μm) of KDP and $Rb_2BiI_5O_{15}$.

Theoretical Calculations

The electronic band structures of the $K_2BiI_5O_{15}$ and $Rb_2BiI_5O_{15}$ crystals are shown in Fig. S9 (ESI†), along the lines of high symmetry points in the Brillouin zone, exhibiting the calculated energy band gaps of 2.51 eV and 2.47 eV, respectively. Both values are smaller than the experimental values of 3.50 eV in $K_2BiI_5O_{15}$ and 3.53 eV in $Rb_2BiI_5O_{15}$. The two crystals are both indirect gap crystals with the energy band gap at G point 0.02 eV ($K_2BiI_5O_{15}$) and 0.04 eV ($Rb_2BiI_5O_{15}$) larger than the indirect gap, respectively. Meanwhile, the partial density of states (PDOS) projected on the constitutional atoms of the title compounds are shown in Fig. S10 (ESI†), from which the following electronic characteristics are shown: (i) The region lower than -8 eV is consisted of the isolated orbitals, which have little interaction with neighbour atoms. (ii) The upper part of VB and the bottom of CB are mainly composed of the p orbitals of oxygen (2p) and iodine (5p), thus the states on the both sides of the band gap mostly consist of those from the I-O group. Since the optical response of a crystal mainly originates from the electronic transitions between the VB and CB states close to the band gap,[20] the I-O group determine the optical properties in both crystals, in accordance with the anionic group theory proposed by Chen[21] for the ultraviolet NLO crystals.

The first-principles linear and nonlinear optical properties in $K_2BiI_5O_{15}$ and $Rb_2BiI_5O_{15}$ are listed in Table 2. The calculated powder SHG effects are in very good agreement with the experimental results, which verifies the validity of the pseudopotential methods employed. Both calculated and experimental values indicate that the two compounds have the relatively large SHG responses to the incident light. Moreover, the relatively large birefringence (Δn) at both the wavelength (λ) of 1064 nm and 2090 nm in $K_2BiI_5O_{15}$ and $Rb_2BiI_5O_{15}$ demonstrates that these two compounds are easy to achieve the phase-matching condition in the IR spectral region. From the point view of structure-property relationship, the large optical anisotropy originates from the ordered arrangement of the long pair electrons on the I-O groups along the z-axis.

Table 2. The calculated linear and nonlinear optical properties in $K_2BiI_5O_{15}$ and $Rb_2BiI_5O_{15}$ crystals

	Refractive indices and birefringence			NLO coefficients (pm/V)	
	λ (nm)	1064	2090		
$K_2BiI_5O_{15}$	n_x	2.1391	2.1189	d_{31}	-0.60
	n_y	2.1268	2.1061	d_{32}	2.73
	n_z	2.0855	2.0674	d_{33}	0.29
	Δ*n*	0.0536	0.0515	Powder SHG	1.7 (~5×KDP)
$Rb_2BiI_5O_{15}$	n_x	2.1338	2.1138	d_{31}	-0.61
	n_y	2.1127	2.0926	d_{32}	2.37
	n_z	2.0911	2.0728	d_{33}	-0.32
	Δ*n*	0.0427	0.0410	Powder SHG	1.4 (~4×KDP)

Thermal properties

The thermal behavior of $K_2BiI_5O_{15}$ and $Rb_2BiI_5O_{15}$ were investigated using thermogravimetric analysis (TGA). The TG curves reveal that they are thermally stable up to about 450 °C (Fig. S11 and S12 ESI†)

Conclusions

In summary, two promising NLO materials, $K_2BiI_5O_{15}$ and $Rb_2BiI_5O_{15}$, have been synthesized by hydrothermal method. They are iso-structural, with the same space group Abm2. They represent first two NCS structure that contains $[I_3O_9]^{3-}$ bridge. Powder second-harmonic generation (SHG) measurements revealed that they belong to the phase-matchable class with a moderate SHG response of approximately 3 times that of KDP. A preliminary measurement indicates that their laser-induced damage thresholds on powders are about 84 and 72 MW/cm^2, respectively, higher than that of $AgGaS_2$. They also exhibit a wide transparent range (up to 12μm) and good thermal stability (450 °C).

Acknowledgements

This work was supported by the National Science Foundation of China (Grant No. 91022036 and 11174297) and the National Key Fundamental Research (973) Program of China (Grant No. 2010CB630701). We thank Prof. Mingliang Tong of Sun Yat-sen University for help with the crystal structure analysis and Prof. Zhanggui Hu of the Technical Institute of Physics and Chemistry, Chinese Academy of Sciences, for help in LDT measurement.

Notes and references

[a] Department of Chemistry, Wuhan University, Wuhan 430072, China, E-mail: jgqin@whu.edu.cn.

[b] College of Chemistry, Central China Normal University, Wuhan 430079, China.

[c] Beijing Center for Crystal R&D, Technical Institute of Physics and Chemistry, Chinese Academy of Sciences, Beijing 100190, China.

† Electronic Supplementary Information (ESI) available: [XRD, EDX, ATR-FTIR, theoretical calculations, and selected bond distances]. See DOI: 10.1039/b000000x/

1 D. M. Burland, R. D. Miller, C. A. Walsh, *Chem. Rev.*, 1994, **94**, 31.

2 (a) C. T. Chen, B. C. Wu, A. D. Jiang, G. M. You, *Sci. Sin. Ser. B*, 1985, 28, 235; (b) C. T. Chen, Y. C. Wu, A. D. Jiang, B. C. Wu, G. M. You, R. K. Li, S. J. Lin, *J. Opt. Soc. Am. B*, 1989, **6**, 616; (c) W. L. Smith, *Appl. Opt.*, 1977, **16**, 798; (d) K. Kato, *IEEE J. Quantum Electron.* 1991, **27**, 1137; (e) G. D. Boyd, R. C. Miller, K. Nassau, W. L. Bond, A. Savage, *Appl. Phys. Lett.* , 1964, **5**, 234.

3 (a) A. O. Okorogu, S. B. Mirov, W. Lee, D. I. Crouthamel, N. Jenkins, A. Y. Dergachev, K. L. Vodopyanov, V. V. Badikov, *Opt .Commun.* , 1998, **155**, 307; (b) D. S. Chemla, P. J. Kupecek, D. S. Robertson, R. C. Smith, *Opt. Commun.*, 1971, **3**, 29; (c) G. D. Boyd, H. M. Kasper, J. H. McFee, F. G. Storz, *IEEE J. Quant .Electron.* , 1972, **8**, 900; (d) G. D. Boyd, E. Buehler, F. G. Storz, *Appl. Phys. Lett.* , 1971, **18**, 301.

4 (a) D. Phanon, I. Gautier-Luneau, *Angew. Chem., Int. Ed.* , 2007, **46**, 8488; (b) K. M. Ok, P. S. Halasyamani, *Angew. Chem., Int. Ed.* , 2004, **116**, 5605; (c) K. M. Ok, P. S. Halasyamani, *Inorg. Chem.* , 2005, 44, 9353; (d) R. E. Sykora, K. M. Ok, P. S. Halasyamani, T. E. Albrecht-Schmitt, *J. Am. Chem. Soc.* , 2002, **124**, 1951; (e) X. Chen, L. Zhang, X. Chang, H. Xue, H. Zang, W. Xiao, X. Song, H. Yan, *J. Alloys Compd.* , 2007, **428**, 54; (f) H. Y. Chang, S. H. Kim, P. S.

Halasyamani, K. M. Ok, *J. Am. Chem. Soc.* , 2009, **131**, 2426; (g) H. Y. Chang, S. H. Kim, K. M. Ok, P. S. Halasyamani, *J. Am. Chem. Soc.* , 2009, 131, 6865; (h) C. F. Sun, C. L. Hu, X. Xu, J. B. Ling, T. Hu, F. Kong, X. F. Long, J. G. Mao, *J. Am. Chem. Soc.* , 2009, **131**, 9486; (i) C. F. Sun, C. L. Hu, X. Xu, B. P. Yang, J. G. Mao, *J. Am. Chem. Soc.* , 2011, **133**, 5561; (j) F. Kong, C. F. Sun, B. P. Yang, J. G. Mao, *Struct Bond,* Springer-Verlag Berlin Heidelberg, 2012, **144**, 43.

5 (a) S. D. Nguyen, J. Yeon, S. H. Kim, P. S. Halasyamani, *J. Am. Chem. Soc.* , 2011, **133**, 12422; (b) Z. Cao, Y. Yue, J. Yao, Z. Lin, R. He, Z. Hu, *Inorg. Chem.* , 2011, **50**, 12818.

6 P. M. Kubelka, F. Z. Munk, *Tech. Phys.* , 1931, **12**, 593.

7 S. K. Kurtz, T. T. Perry, *J. Appl. Phys.* , 1968, **39**, 3798.

8 (a) M. J. Zhang, X. M. Jiang, L. J. Zhou, G. C. Guo, *J. Mater. Chem. C*, 2013, **1**, 4754; (b) M. J. Zhang, B. X. Li, B. W. Liu, Y. H. Fan, X. G Li, H. Y. Zeng, G. C. Guo, *Dalton Trans.*, 2013, **42**, 14223.

9 G. M. Sheldrick, *SHELXTL*, Version 6.14; Bruker Analytical X-ray Instruments, Inc., Madison, WI, USA, **2003**.

10 G. M. Sheldrick, *Acta Cryst.*, 2008, **A64**, 112.

11 M. C. Payne, M. P. Teter, D. C. Allan, T. A. Arias, J. D. Joannopoulos, *Rev. Mod. Phys.* , 1992, **64**, 1045.

12 S. J. Clark, M. D. Segall, C. J. Pickard, P. J. Hasnip, M. J. Probert, K. Refson, M. C. Payne, *Z. Kristallogr.* , 2005, **220**, 567.

13 J. S. Lin, A. Qteish, M. C. Payne, V. Heine, *Phys. Rev. B*, 1993, **47**, 4174.

14 L. Kleinman, D. M. Bylander, *Phys. Rev. Lett.* , 1982, **48**, 1425.

15 J. P. Perdew, K. Burke, Y. Wang, *Phys. Rev. B.* ,1996, **54**, 16533.

16 H. J. Monkhorst, J. D. Pack, *Phys. Rev. B.* , 1976, **13**, 5188.

17 E. D. Palik, *Handbook of Optical Constants of Solids*, Academic Press, **1985**, 190.

18 J. Lin, M. H. Lee, Z. P. Liu, C. T. Chen, C. J. Pickard, *Phys. Rev. B.* , 1999, **60**, 13380.

19 (a) C. S. Wang, B. M. Klein, *Phys. Rev. B.* , 1981, **2**, 3393; (b) R. W. Godby, M. Schluter, L. J. Sham, *Phys. Rev. B.* , 1988, **37**, 10159.

20 M. H. Lee, C. H. Yang, J. H. Jan, *Phys. Rev. B.* , 2004, **70**, 235110.

21 C. T. Chen, T. Sasaki, R. K. Li, Y. C. Wu, Z. S. Lin, Y. Mori, Z. G. Hu, J. Y. Wang, G. Aka, M. Yoshimura, Y. Kaneda, *Nonlinear Optical Borate Crystals.* Wiley-VCH, Germany, **2012**.

